

# The importance of being stable: the role of stability conditions in single field Quintessence

Simone Peirone,<sup>1</sup> Matteo Martinelli,<sup>1</sup> Marco Raveri,<sup>2,1</sup> and Alessandra Silvestri<sup>1</sup>

<sup>1</sup>*Institute Lorentz, Leiden University, PO Box 9506, Leiden 2300 RA, The Netherlands*

<sup>2</sup>*Kavli Institute for Cosmological Physics, Enrico Fermi Institute,  
The University of Chicago, Chicago, Illinois 60637, USA*

We investigate the impact of general conditions of theoretical stability and cosmological viability on dynamical dark energy models. As a powerful example, we study whether minimally coupled, single field Quintessence models that are safe from ghost instabilities, can source the CPL expansion history recently shown to be mildly favored by a combination of CMB (Planck) and Weak Lensing (KiDS) data. Interestingly we find that in their most conservative form, the theoretical conditions impact the analysis in such a way that smooth single field Quintessence becomes significantly disfavored with respect to the standard  $\Lambda$ CDM cosmological model. This is due to the fact that these conditions cut a significant portion of the  $(w_0, w_a)$  parameter space for CPL, in particular eliminating the region that would be favored by weak lensing data. Within the scenario of a smooth dynamical dark energy parametrized with CPL, weak lensing data favors a region that would require multiple fields to ensure gravitational stability.

## I. INTRODUCTION

Recent observational results from weak lensing experiments [1, 2] have been found to be in substantial discordance with cosmic microwave background measurements from Planck [3].

This discordance is usually quantified by means of consistency tests [4–7] or in terms of the  $S_8 = \sigma_8 \sqrt{\Omega_m/0.3}$  derived parameter, to which weak lensing surveys are expected to be particularly sensitive [8].

In particular, in the case of the Kilo Degree Survey (KiDS), this discordance is measured to be at the level of  $2.3\sigma$  [2].

As a first attempt at overcoming the tension between these data sets, the effects of systematics on the measurements of both weak lensing [2, 7, 8] and Planck [9] have been extensively studied. Despite significant effort, no relevant reduction of the tension has been found so far. Therefore, it looks reasonable to investigate whether this discordance is due to the assumption of the standard cosmological model,  $\Lambda$ CDM. For some recent work in this direction see [10, 11]

In a recent paper [8], the authors explored this avenue, by looking at some simple extensions of the  $\Lambda$ CDM model, such as massive neutrinos, a model with non-zero curvature contribution, and some simple dynamical dark energy (DE) models parametrized through a constant equation of state  $w \neq -1$  as well as the time-varying one  $w(a) = w_0 + w_a(1-a)$  introduced by Chevallier-Polarski-Linder (CPL) [12, 13]. As result of their analysis, the authors found that the only model which alleviates the tension and which is favored by the combined KiDS and Planck datasets, from a bayesian model selection point of view, is a CPL-parametrized Dark Energy model, which indeed reduces the tension on  $S_8$  to  $0.91\sigma$  [8].

Given this interesting result, in this paper we ask which *theoretically viable* DE model could correspond to the expansion history required to solve the tension between

KiDS and Planck data. In [8] the analysis was performed using the Parametrized Post Friedmann (PPF) approach [14, 15], which allows to broadly explore the parameter space of the CPL parametrization while keeping the perturbations of DE well behaved. However, when interpreting the results, it is worth remembering that the region corresponding to  $w < -1$  cannot be linked to single field minimally coupled quintessence models, since the latter suffer from ghost instabilities for those values of the equation of state [16–18]. As we will elaborate in Section II, within the PPF approach, the  $w < -1$  region necessarily corresponds to multifield scenarios, where the additional degrees of freedom ensure gravitational stability.

The paper is organized as follows. In Section II we revisit general conditions of stability for DE models, focusing on minimally coupled quintessence. We then describe how we implement these conditions in our exploration of CPL models. In Section III we describe the data sets that we employ and, finally, we show the results of our analysis in Section IV. We draw our Conclusions in Section V.

## II. DYNAMICAL DARK ENERGY: STABILITY AND VIABILITY CONDITIONS

In the analysis of observational data it is often useful to explore broad classes of models through a framework that parametrizes the relevant deviations from the standard  $\Lambda$ CDM cosmological model. This approach is commonly applied to the investigation of dynamical DE models, where the equation of state is often described by the CPL parametrization [19, 20]:

$$w_{\text{DE}}(a) = w_0 + w_a(1 - a). \quad (1)$$

When going beyond background probes, the latter is commonly combined with the Parametrized Post-Friedmann (PPF) framework for DE perturbations, in-

troduced in [14, 21] and implemented in the Einstein-Boltzmann solver **CAMB** in [15]. This offers a stable and accurate description of DE perturbations over the entire parameter space of CPL, provided that the DE field remains smooth with respect to matter on the scales of interest.

While adopting a parametrized framework, it is informative to make contact with known theories and associate different regions of the parameter space to different viable classes of theories. In the following, we shall argue that the CPL parametrization, combined with the PPF module, can represent stable single field, minimally coupled quintessence only in the  $(w_0, w_a)$  region corresponding to  $w > -1$ . Outside of that range, results need to be interpreted within the realm of multifield DE.

Minimally coupled, single field models with a speed of sound equal to unity, are arguably the simplest models of dynamical DE. We will refer to them as *standard quintessence*. For these models, the DE field remains smooth on sub-horizon scales, and PPF offers an accurate prescription. However, in this case one should be careful with the allowed regions of the parameter space  $(w_0, w_a)$ . Indeed, these models would generally suffer from ghost instabilities for  $w < -1$  [17, 22–24]. These instabilities arise from the wrong sign of the kinetic term, which translates into an Hamiltonian unbounded from below and, thus, into an unstable quantum vacuum. Correspondingly,  $w = -1$  is referred to as the *phantom divide* and single field models crossing through it are gravitationally unstable.

As explored in [16], while it is difficult, it is not impossible to have a quintessence model with  $w < -1$  which is *effectively* stable, i.e. the rate of the instabilities is longer than the time scale of interest for the analysis. We keep this option open, as we will elaborate shortly, however we will see that requiring that no instabilities develop over the relevant time interval will still cut a significant portion of the  $w < -1$  region.

Alternatively, single field DE models could safely cross the phantom divide if the DE field was non minimally coupled to gravity [25] or the model included higher order derivative operators, as discussed in [17]. However, in the former case, the DE component would be clustering and in the latter case, as shown in [17], stability requires that in the region  $w < -1$  the DE field behaves like a k-essence fluid with an approximately zero speed of sound. As such, in both these cases, the DE component cannot be considered smooth on the scales of relevance for large scale structure surveys, and hence the PPF framework does not apply.

Which DE models could then correspond to CPL models with  $w < -1$  and for which the DE field remains relatively smooth with respect to matter, (so that PPF is an accurate prescription)? As discussed in [14, 21], one necessarily needs to dwell into the multifield scenarios, with additional degrees of freedom ensuring gravitational stability. This is the assumption at the heart of the PPF approach.

In summary, data analysis that employ the CPL parametrization, and its implementation in **CAMB** through the PPF module, can correspond to single field quintessence only when  $w \geq -1$ ; regions where  $w < -1$ , should be interpreted more broadly in terms of multiple fields. There remains the possibility that part of the prohibited region can still be *effectively* stable for standard quintessence. However, such area of the parameter space should be determined and the corresponding cut should be applied to the data analysis if one wants to interpret results within the realm of standard quintessence.

In this work we shall assess the importance of stability requirements and their impact on the results obtained with the CPL parametrization, by performing the same analysis of [8] within the realm of standard quintessence. This will allow us to determine whether the CPL model favored by data in [8], can correspond to standard quintessence or shall be interpreted in a broader framework such as that of multiple field DE.

To this extent, we do not employ the PPF approach of **CAMB**, but rather use the minimal implementation of CPL in **EFTCAMB** [26, 27], which corresponds to a designer standard quintessence with CPL expansion history. The key feature of this latter approach, relies in the check for the stability of the theory which is built-in in **EFTCAMB**. Specifically, **EFTCAMB** has a stability module which imposes two sets of conditions: Mathematical stability Conditions (MC) and Physical stability Conditions (PC). The former are general conditions which do not rely on any theoretical assumption, and ensure mathematical consistency and numerical stability of perturbations in the DE sector. They include conditions for:

- the well-posedness of the scalar field perturbations initial value problem;
- the avoidance of exponential growth of the quintessence field perturbations;
- the existence of a viable cosmological background with matter and radiation eras and an accelerated phase ( $w_{\text{DE}} < -1/3$ ).

On the other hand, PC enforce the absence of ghost and gradient instabilities. Since we put ourselves in the case of a CPL standard quintessence, the stability check will automatically ensure that we do not explore regions of  $(w_0, w_a)$  that would correspond to an unstable model.

While MC and PC can be turned on and off independently, in our analysis we use either MC or the full combination of the two (FC), in order to provide a full protection against instabilities. We stress that a more complete set of PC, e.g. including no-tachyon conditions [28], is being worked out.

In Fig. 1 we show the effect of MC and FC on the CPL parameter space,  $(w_0, w_a)$ , within the realm of standard quintessence. As we can see in Panel a) MC prohibit the crossing of  $w = -1$ , cutting a relevant portion of parameter space, since that would lead to an ill posed initial value problem for minimally coupled single field

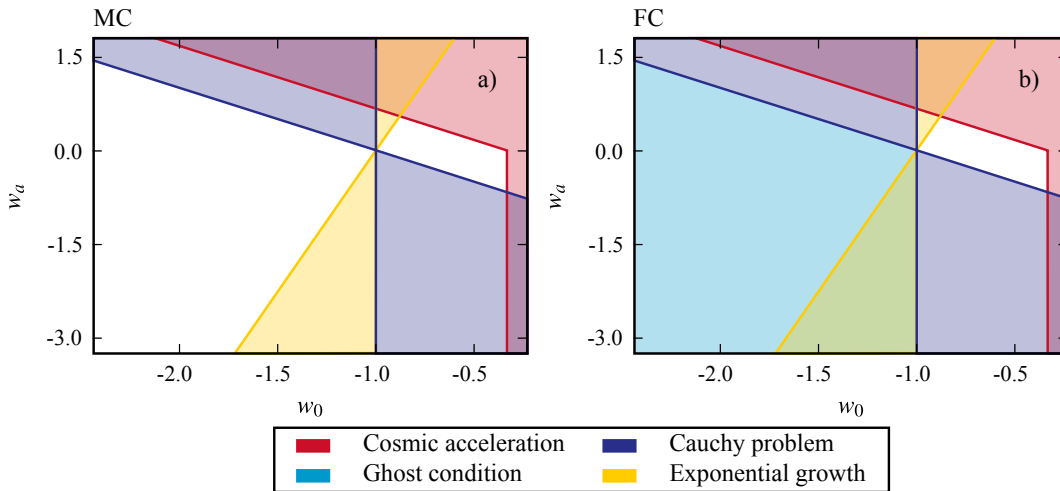


FIG. 1. Viable and non-accessible regions of the CPL parameter space within the realm of *standard quintessence*. Different colors correspond to different viability and stability conditions, as shown in legend. In the *left* panel we show the effects of Mathematical Conditions (MC): the blue regions are prohibited by requiring the well-posedness of the scalar field perturbations initial value problem; the red ones by the existence of a viable cosmological background; the yellow ones by the avoidance of exponential growth of the DE perturbations. In the *right* panel, we show the full combination (FC) of mathematical and physical conditions. The only additional cut is the one imposed by the no-ghost condition, shown in light blue.

quintessence perturbations. On the other hand, as shown in Panel b), the only cut introduced by PC is the one coming from the no-ghost condition, which cuts the portion of the parameter space corresponding to  $w < -1$  at all times. Comparing the two panels, we can see that MC allow some parts of the  $w < -1$  region, namely those for which the instabilities are still there (from the theoretical point of view), but do not affect the observables, i.e. they do not develop over the relevant time range.

In this paper we compare our results for CPL quintessence under MC and FC, with those of [8], where the PPF module was used.

The results of our analysis, which we present in Section IV, will show how much impact MC and FC can have on the final results and will serve us as an example to stress the power of theoretical stability and viability conditions in the analysis of cosmological data.

### III. DATA ANALYSIS

Following [8], we consider the full set of data from the tomographic weak gravitational lensing analysis of  $\sim 450\text{deg}^2$  by the four-band imaging Kilo Degree Survey (KiDS) [2, 29, 30], including baryonic effects in the non-linear matter power spectrum with HMCODE [31], which is already incorporated in CAMB. In addition, we also consider the Planck measurements [9, 32] of CMB temperature and polarization on large angular scales, limited to multipoles  $\ell \leq 29$  (low- $\ell$  TEB likelihood) and the CMB temperature on smaller angular scales (PLIK TT likelihood). Since we are interested in comparing our results with [8], we will not consider Planck polarization

measurements on smaller angular scales as well as Planck CMB lensing measurements.

We use EFTCAMB and EFTCosmoMC [26, 27], modifications of the CAMB/CosmoMC codes [33, 34], and we implement these in the version of CosmoMC made publicly available by the KiDS collaboration [8]. We analyze KiDS and Planck both separately and combining them, sampling the standard cosmological parameters, i.e. the baryon and cold dark matter energy densities  $\Omega_b h^2$  and  $\Omega_c h^2$ , the optical depth at reionization  $\tau$ , the amplitude and tilt of primordial power spectrum  $\ln 10^{10} A_s$  and  $n_s$  and the angular size of the sound horizon at last scattering surface  $\theta$ . To these we add the CPL parameters  $w_0$  and  $w_a$  when we analyze the extension to the  $\Lambda$ CDM model, and we perform this analysis both in the MC and FC cases. Furthermore, as done in [2, 8], we include, as free parameters, the amplitude of intrinsic alignments  $A_{IA}$  and the amplitude of baryonic feedback  $B$ . We adopt flat priors on the sampled parameters, with the same prior ranges defined in Table 1 of [8], using the standard case for the systematic parameters  $A_{IA}$  and  $B$ .

In order to assess the effect of the conditions on the possibility of reducing the low-high redshift tension with a dynamical Dark Energy, we exploit the same statistical tools used in [8]; this will allow us to compare our results to the standard PPF treatment of a dynamical Dark Energy. We therefore consider the tension between Planck (P) and KiDS (K) datasets on the  $S_8 = \sigma_8 \sqrt{\Omega_m/0.3}$  parameter, defining it as

$$T(S_8) = \frac{|S_8^P - S_8^K|}{\sqrt{\sigma^2(S_8^P) + \sigma^2(S_8^K)}}. \quad (2)$$

We also assess the preference of the data for any of the

considered models over  $\Lambda$ CDM computing the *Deviance Information Criterion* (DIC) [35]:

$$\text{DIC} \equiv \chi_{\text{eff}}^2(\hat{\theta}) + 2p_D, \quad (3)$$

with  $\chi_{\text{eff}}^2(\hat{\theta}) = -2 \ln \mathcal{L}(\hat{\theta})$ ,  $\hat{\theta}$  the parameters vector at the maximum likelihood and  $p_D = \overline{\chi_{\text{eff}}^2(\theta)} - \chi_{\text{eff}}^2(\hat{\theta})$ , where the bar denotes the average taken over the posterior distribution. The DIC accounts both for the goodness of fit through  $\chi_{\text{eff}}^2(\hat{\theta})$  and for the bayesian complexity of the model,  $p_D$ , which disfavours more complex models. When comparing  $\Lambda$ CDM with its extension (ext), we compute:

$$\Delta \text{DIC} = \text{DIC}_{\text{ext}} - \text{DIC}_{\Lambda\text{CDM}}. \quad (4)$$

From this definition it follows that a negative  $\Delta \text{DIC}$  would support the extended model, while a positive one would support  $\Lambda$ CDM. Finally, we exploit the DIC to assess the concordance of the two different datasets as [7]

$$\log \mathcal{I} = -\frac{\mathcal{G}(P, K)}{2}, \quad (5)$$

with  $\mathcal{G}$  defined as

$$\mathcal{G}(P, K) \equiv \text{DIC}(P \cup K) - \text{DIC}(P) - \text{DIC}(K), \quad (6)$$

where  $P \cup K$  denotes the combination of Planck and KiDS datasets.

#### IV. RESULTS

In this section we report the results obtained with the analysis described in section III. We do not report the results on all the cosmological parameters, but rather focus on the quantities introduced above to quantify the tension between the datasets and to assess the effects of the theoretical conditions on it.

The left panel of Fig. 2 shows the constraints obtained in the  $\sigma_8 - \Omega_m$  plane analyzing Planck data assuming  $\Lambda$ CDM and CPL quintessence with the two possible conditions applied to the model.

We notice that applying MC qualitatively preserves the behavior of the CPL analysis with the PPF approach [8], allowing for smaller values of  $\Omega_m$ . Adopting the FC instead, moves the contours toward higher  $\Omega_m$  values. This difference is due to the change in the allowed  $w_{\text{DE}}$  values, as can be seen in the right panel of Figure 2. The analysis with MC disfavors the  $w_{\text{DE}} > -1.0$  region, while the analysis with FC is constrained to be in the  $w_{\text{DE}} > -1.0$  region. Secondly, we see that the FC are much more effective in constraining the  $w_a$  parameter as the geometric degeneracy between  $w_0$  and  $w_a$  is broken by viability conditions. This leads to tighter constraints also in the  $\sigma_8 - \Omega_m$  plane.

Given this behavior, we expect the CPL quintessence, with MC, to preserve the ability to ease the tension between Planck and KiDS data. This is indeed the case,

	$T(S_8)$	$\log \mathcal{I}$
$\Lambda$ CDM	$2.3\sigma$	-0.48
CPL + MC	$1.0\sigma$	0.97
CPL + FC	$1.3\sigma$	-0.76

TABLE I. Tension ( $T$ ) and concordance ( $\log \mathcal{I}$ ) parameters between KiDS and Planck data in  $\Lambda$ CDM and in CPL with MC and with FC.

	$\Delta \chi_{\text{eff}}^2$	$\Delta \text{DIC}$
CPL + MC		
KiDS	-0.02	3.2
Planck	-2.9	-2.0
Planck+KiDS	-5.4	-5.4
CPL + FC		
KiDS	-0.3	0.2
Planck	1.6	3.2
Planck+KiDS	1.0	4.6

TABLE II. Model comparison through the obtained values of  $\Delta \chi_{\text{eff}}^2$  and  $\Delta \text{DIC}$  using as a reference  $\chi_{\text{eff}}^2$  the one obtained in a  $\Lambda$ CDM analysis.

as can be seen in the left panel of Figure 3 and from Table I. Following the hierarchy discussed in [8], the values  $T(S_8) = 1$  and  $\log \mathcal{I} = 0.97$  highlight how the tension is removed and the two datasets are now in substantial concordance. The right panel of Figure 3 shows the constraints on  $w_0$  and  $w_a$ . Notice that when the two datasets are combined a deviation of more than  $2\sigma$  from the  $\Lambda$ CDM model is found. Computing then  $\Delta \text{DIC}$  results in a moderate preference of the data for the CPL model when combining Planck and KiDS (see Table II). As expected these results are in agreement with those obtained using a PPF approach [8].

The left panel of Figure 4 shows instead the constraints achieved when FC are used in the analysis. As discussed above, in this case the Planck data prefer higher values of  $\Omega_m$ . Even though the tension with KiDS data on the  $S_8$  parameter is eased with respect to the  $\Lambda$ CDM case ( $T(S_8) = 1.3$ ), the concordance between the two datasets is worsened ( $\log \mathcal{I} = -0.76$ ). As shown in the right panel of Figure 4, in this case the constraints on  $w_0$  and  $w_a$  are compatible with  $\Lambda$ CDM  $w = -1$ ; additionally, as can be seen in Table II, the CPL model is disfavored with respect to  $\Lambda$ CDM when we account for FC ( $\Delta \text{DIC} = 4.6$  when the two datasets are combined) because the fit does not improve significantly over the  $\Lambda$ CDM one while the parameter space dimension grows. This is due to the fact that the  $w(z) < -1.0$  region, which is the one favorite by the data in KiDS analysis, is here completely removed by the FC, as physically viable single field quintessence models are not able to reproduce this evolution.

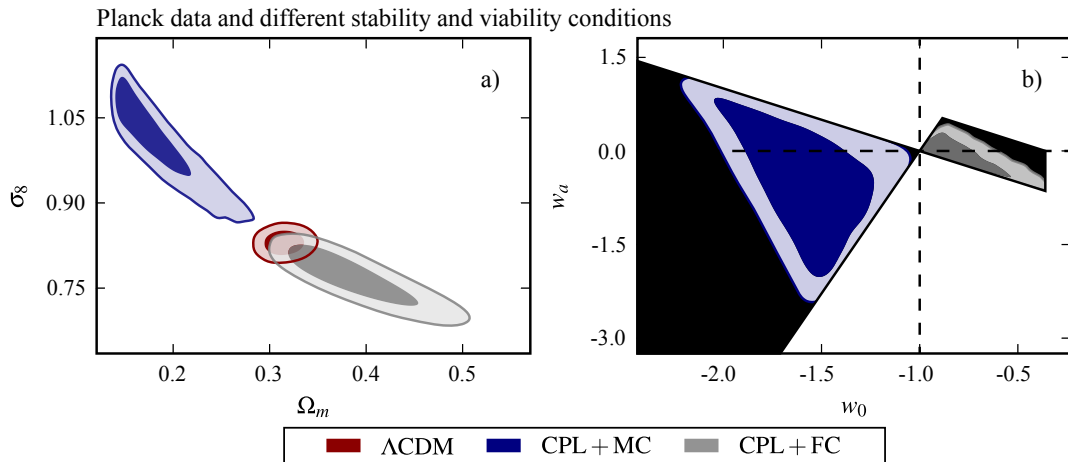


FIG. 2. The joint marginalized posterior of  $\Omega_m$  and  $\sigma_8$  (panel a) and  $w_0$  and  $w_a$  (panel b) as obtained with the Planck data in  $\Lambda$ CDM (red contours), CPL with MC (blue contours) and with FC (gray contours). The darker and lighter shades correspond respectively to the 68% C.L. and the 95% C.L. regions. The dashed line indicates the point corresponding to the  $\Lambda$ CDM model in the  $w_0 - w_a$  plane.

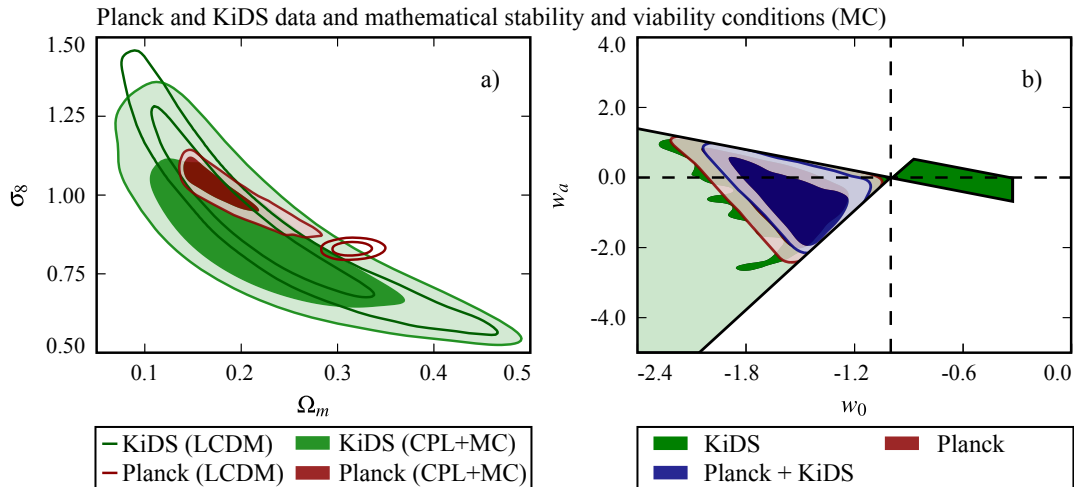


FIG. 3. The joint marginalized posterior of  $\Omega_m$  and  $\sigma_8$  (panel a) and  $w_0$  and  $w_a$  (panel b) as obtained analyzing KiDS (green contours) and Planck (red contours) data. Filled contours refer to constraints obtained in CPL with MC, while empty contours (left panel only) refer to  $\Lambda$ CDM constraints. The darker and lighter shades correspond respectively to the 68% C.L. and the 95% C.L. regions. The dashed line indicates the point corresponding to the  $\Lambda$ CDM model in the  $w_0 - w_a$  plane.

## V. CONCLUSIONS

In this work we revisited the interesting possibility of easing the tension between weak lensing and CMB data with a dynamical dark energy, whose equation of state is described by the CPL parametrization, in light of the results of [8]. In particular, we explored whether the model favored by Planck and KiDS data in [8] could correspond to a theoretically viable single field quintessence, by restricting the parameter space of CPL to that corresponding to *stable standard quintessence*. With the latter, we indicate DE models corresponding to one scalar field minimally coupled to gravity and without higher

order derivative operators. This theoretical assumption leads to restrictions on the allowed parameter space of the CPL parametrization, as described in Section II. In order to study the impact of these conditions on the observational constraints, we performed an analysis analogous to the one done in [8], using the theoretical conditions of stability and viability built-in in EFTCAMB.

We considered two types of conditions: Mathematical (MC) and the Physical Stability Conditions (PC). The former are rather generic and consider only the numerical stability of the model, without any theoretical consideration. The latter are more restrictive, ruling out all models with ghost or gradient instabilities on the basis of

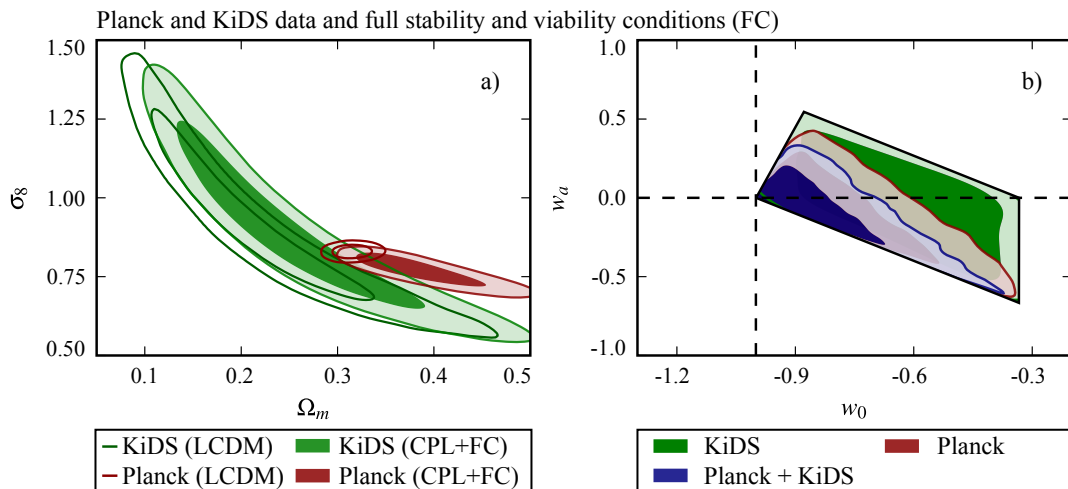


FIG. 4. The joint marginalized posterior of  $\Omega_m$  and  $\sigma_8$  (panel a) and  $w_0$  and  $w_a$  (panel b) as obtained analyzing KiDS (red contours) and Planck (blue contours) data. Filled contours refer to constraints obtained in CPL with FC, while empty contours (left panel only) refer to  $\Lambda$ CDM constraints. The darker and lighter shades correspond respectively to the 68% C.L. and the 95% C.L. regions. The dashed line indicates the point corresponding to the  $\Lambda$ CDM model in the  $w_0 - w_a$  plane.

theoretical considerations [16, 17]. One convenient way to compare these two classes of conditions is to look at the corresponding parameter space in the  $(w_0, w_a)$ -plane. While MC allow for the phantom divide crossing, the full set, FC, strictly forbids the region corresponding to  $w < -1$ , since for smooth single field quintessence ghost instabilities would develop. These instabilities could be avoided with the inclusion of higher order derivative operators or additional degrees of freedom in the dark sector, but in both cases we would move away from single field, relatively smooth quintessence [14, 17].

After performing a fit to KiDS and Planck data by means of EFTCosmoMC, we find that in the MC case, even though the allowed parameter space is shrunk with respect to the PPF case, the expansion history found in [8] and able to ease the  $S_8$  tension is still allowed by the implemented conditions. Therefore, CPL under MC conditions in our implementation yields results analogous to the general PPF case. In particular we find  $\Delta DIC = -5.4$ , showing a moderate preference of the data for the model. Interestingly, the result changes when we apply the FC: in this case, the parameter space of CPL is significantly reduced and both KiDS and Planck contours move towards higher values of  $\Omega_m$ , as shown in Fig. 2, with the net effect of decreasing the tension parameter to  $T(S_8) = 1.3\sigma$ . However, the value of  $\Delta DIC = 4.6$  (for Planck + KiDS) shows that the model is disfavored with respect to  $\Lambda$ CDM.

The tantalizing conclusion of our analysis is that,

the CPL expansion history favored by Planck+KiDS data per [8], cannot correspond to stable single field quintessence, but rather invokes multiple field models with the DE d.o.f. remaining relatively smooth with respect to dark matter. If one indeed restricts to standard quintessence and invokes conditions of theoretical stability,  $\Lambda$ CDM remains a better fit to the data. We leave for future work the exploration of the tension between Planck and KiDS data sets in more general models of dark energy, e.g. stable and viable Horndeski models.

## ACKNOWLEDGMENTS

We thank Noemi Frusciante, Wayne Hu, Massimo Viola for useful discussions and comments, and Shahab Joudaki for clarifications about the implementation of KiDS dataset. SP and AS acknowledge support from The Netherlands Organization for Scientific Research (NWO/OCW), and from the D-ITP consortium, a program of the Netherlands Organisation for Scientific Research (NWO) that is funded by the Dutch Ministry of Education, Culture and Science (OCW). MM acknowledge by the Foundation for Fundamental Research on Matter (FOM) and the Netherlands Organization for Scientific Research / Ministry of Science and Education (NWO/OCW). MR is supported by U.S. Dept. of Energy contract DE-FG02-13ER41958.

[1] T. D. Kitching *et al.* (CFHTLenS), *Mon. Not. Roy. Astron. Soc.* **442**, 1326 (2014), arXiv:1401.6842 [astro-

ph.CO].

- [2] H. Hildebrandt *et al.*, (2016), [arXiv:1606.05338 \[astro-ph.CO\]](#).
- [3] R. Adam *et al.* (Planck), *Astron. Astrophys.* **594**, A1 (2016), [arXiv:1502.01582 \[astro-ph.CO\]](#).
- [4] M. Raveri, *Phys. Rev.* **D93**, 043522 (2016), [arXiv:1510.00688 \[astro-ph.CO\]](#).
- [5] S. Seehars, S. Grandis, A. Amara, and A. Refregier, *Phys. Rev.* **D93**, 103507 (2016), [arXiv:1510.08483 \[astro-ph.CO\]](#).
- [6] S. Grandis, S. Seehars, A. Refregier, A. Amara, and A. Nicola, *JCAP* **1605**, 034 (2016), [arXiv:1510.06422 \[astro-ph.CO\]](#).
- [7] S. Joudaki *et al.*, (2016), 10.1093/mnras/stw2665, [arXiv:1601.05786 \[astro-ph.CO\]](#).
- [8] S. Joudaki *et al.*, (2016), [arXiv:1610.04606 \[astro-ph.CO\]](#).
- [9] N. Aghanim *et al.* (Planck), *Astron. Astrophys.* **594**, A11 (2016), [arXiv:1507.02704 \[astro-ph.CO\]](#).
- [10] J. Hamann and J. Hasenkamp, *JCAP* **1310**, 044 (2013), [arXiv:1308.3255 \[astro-ph.CO\]](#).
- [11] E. Di Valentino, A. Melchiorri, and J. Silk, *Phys. Rev.* **D92**, 121302 (2015), [arXiv:1507.06646 \[astro-ph.CO\]](#).
- [12] M. Chevallier and D. Polarski, *International Journal of Modern Physics D* **10**, 213 (2001), [gr-qc/0009008](#).
- [13] E. V. Linder, *Physical Review Letters* **90**, 091301 (2003), [astro-ph/0208512](#).
- [14] W. Hu and I. Sawicki, *Phys. Rev.* **D76**, 104043 (2007), [arXiv:0708.1190 \[astro-ph\]](#).
- [15] W. Fang, W. Hu, and A. Lewis, *Phys. Rev.* **D78**, 087303 (2008), [arXiv:0808.3125 \[astro-ph\]](#).
- [16] S. M. Carroll, M. Hoffman, and M. Trodden, *Phys. Rev.* **D 68**, 023509 (2003), [astro-ph/0301273](#).
- [17] P. Creminelli, G. D'Amico, J. Noreña, and F. Vernizzi, *JCAP* **2**, 018 (2009), [arXiv:0811.0827](#).
- [18] M. Kunz and D. Sapone, *Phys. Rev.* **74**, 123503 (2006), [astro-ph/0609040](#).
- [19] M. Chevallier and D. Polarski, *Int. J. Mod. Phys.* **D10**, 213 (2001), [arXiv:gr-qc/0009008 \[gr-qc\]](#).
- [20] E. V. Linder, *Phys. Rev. Lett.* **90**, 091301 (2003), [arXiv:astro-ph/0208512 \[astro-ph\]](#).
- [21] W. Hu, *Phys. Rev.* **D77**, 103524 (2008), [arXiv:0801.2433 \[astro-ph\]](#).
- [22] A. Vikman, *Phys. Rev.* **71**, 023515 (2005), [astro-ph/0407107](#).
- [23] W. Hu, *Phys. Rev.* **71**, 047301 (2005), [astro-ph/0410680](#).
- [24] R. R. Caldwell and M. Doran, *Phys. Rev.* **72**, 043527 (2005), [astro-ph/0501104](#).
- [25] S. M. Carroll, A. D. Felice, and M. Trodden, *Phys. Rev.* **71**, 023525 (2005), [astro-ph/0408081](#).
- [26] B. Hu, M. Raveri, N. Frusciante, and A. Silvestri, *Phys. Rev.* **D89**, 103530 (2014), [arXiv:1312.5742 \[astro-ph.CO\]](#).
- [27] M. Raveri, B. Hu, N. Frusciante, and A. Silvestri, *Phys. Rev.* **D90**, 043513 (2014), [arXiv:1405.1022 \[astro-ph.CO\]](#).
- [28] N. Frusciante, G. Papadomanolakis, and A. Silvestri, *JCAP* **7**, 018 (2016), [arXiv:1601.04064 \[gr-qc\]](#).
- [29] J. T. A. de Jong, G. A. Verdoes Kleijn, K. H. Kuijken, and E. A. Valentijn, *Experimental Astronomy* **35**, 25 (2013), [arXiv:1206.1254](#).
- [30] K. Kuijken *et al.*, *Mon. Not. Roy. Astron. Soc.* **454**, 3500 (2015), [arXiv:1507.00738 \[astro-ph.CO\]](#).
- [31] A. J. Mead, J. A. Peacock, C. Heymans, S. Joudaki, and A. F. Heavens, *MNRAS* **454**, 1958 (2015), [arXiv:1505.07833](#).
- [32] P. A. R. Ade *et al.* (Planck), *Astron. Astrophys.* **594**, A13 (2016), [arXiv:1502.01589 \[astro-ph.CO\]](#).
- [33] A. Lewis, A. Challinor, and A. Lasenby, *Astrophys. J.* **538**, 473 (2000), [arXiv:astro-ph/9911177 \[astro-ph\]](#).
- [34] A. Lewis and S. Bridle, *Phys. Rev.* **D66**, 103511 (2002), [arXiv:astro-ph/0205436 \[astro-ph\]](#).
- [35] D. J. Spiegelhalter, N. G. Best, B. P. Carlin, and A. van der Linde, *Journal of the Royal Statistical Society: Series B (Statistical Methodology)* **76**, 485 (2014).